Static recording characteristics of new type super-resolution near-field structure

Feng Zhang (张 锋), Wendong Xu (徐文东), Yang Wang (王 阳), Jinsong Wei (魏劲松), Fei Zhou (周 飞), Xiumin Gao (高秀敏), and Fuxi Gan (干福熹)

Shanghai Institute of Optics and Fine Mechanics, Chinese Academy of sciences, Shanghai 201800

Received May 19, 2004

A novel super-resolution near-field optical structure (super-RENS) with bismuth (Bi) mask layer is proposed in this paper. Static optical recording tests with and without super-RENS are carried out using a 650-nm semiconductor laser at recording powers of 14 and 7 mW with pulse duration of 100 ns. The recording marks are observed by high-resolution optical microscopy with a charge-coupled device (CCD) camera. The results show that the Bi mask layer can also concentrate energy into the center of a laser beam at low laser power similar to the traditional Sb mask layer. The results above are further confirmed by another Ar^+ laser system. The third-order nonlinear response induced by the plasma oscillation at the Bi/SiN interface during laser irradiation can be used to explain the phenomenon. The calculation results are basically consistent with our experimental results.

OCIS codes: 160.4330, 210.0210, 310.0310.

Optical near-field recording (NFR) technologies have been studied for approximately 20 years with the aim of overcoming the diffraction limit in super-high-density optical storage[1,2]. Among them, super-resolution near-field structure (super-RENS), with a typical structure of SiN/Sb(15 nm)/SiN, which was first proposed by Tominaga *et al.*[1], is one of the most promising schemes because it does not use any flying NFR heads or system that maintains a nanometer spacing between the NFR head and recording medium. Attention has been focused on the working mechanism of TA-type super-RENS (also called Sb-super-RENS because Sb was used as the mask layer material). It was originally considered to be a photothermally induced phase change between crystalline and melted states of Sb thin film under a focused laser beam[3]. Later, direct near-field measurement of Sb-super-RENS was reported by Tsai *et al.*[4] and localized surface plasma effects of the super-RENS were observed. Recently, a nonlinear semiconductor model[5] and thermal lens model[6] had been proposed to explain the working mechanism of the super-RENS. According to these explanation, new near-field active mask layer materials of super-RENS is proposed.

Bi has been the subject of many studies because it shows special properties in the thin-film form. Such films were reported to show superconductivity[7], large magneto-resistance[8], quantum size effects[9], and nonlinear optical properties[10]. Pan *et al.*[11] found that silica glasses implanted with Bi particles have larger nonlinear index than those implanted with Sb particles. Recently, Liu *et al.* have found that thin Bi films have unusually giant third-order optical nonlinearity at low laser intensity, which is $\sim 10^5$ times larger than that of composites containing Bi nanoparticles[12]. The giant nonlinearity of Bi thin films may be useful for the energy concentration of the laser beam and the size reduction of recording marks. The third-order nonlinear response induced by the plasma oscillation at the Bi/SiN interface during laser irradiation can be used to explain the phenomenon.

In our experiments, four specimens were prepared. Specimen 1 was single-layer Bi films with thickness of 10 nm sputtered on K9 glass plates (1.2 mm) for atomic force microscopy (AFM) (AJ-III, AJ Nano Science Co.) and grazing incident X-ray diffraction (XRD) (D/max 2550 V, RIGAKU Co.) studies. Specimens 2 and 3 were multi-layer with structures of cover glass(0.13 mm)/SiN(10 nm)/Sb(10 nm)/SiN (10 nm)/$Ge_2Sb_2Te_5$(10 nm), cover glass(0.13 mm)/SiN (10 nm)/Bi(10 nm)/SiN(10 nm)/$Ge_2Sb_2Te_5$(10 nm), respectively (as shown in Fig. 1). Specimen 4 was a single-layer $Ge_2Sb_2Te_5$ film with thickness of 10 nm sputtered on cover glass (0.13 mm). Specimens 2, 3, and 4 were used for static recording tests, scanning electron microscope (SEM) (JSM-6360LA, JEOL CO.), and optical microscopy studies, respectively. In our experiments, all the films were prepared by radio-frequency magnetron sputtering on cleaned substrates at the background pressure of less than 1.0×10^{-4} Pa. A 650-nm semiconductor laser beam after shaping and Ar^+ laser through a high numerical aperture (NA) (0.85) objective lens was used to record marks of less than 1 μm in diameter. The recording marks were observed and studied by SEM or high-resolution optical microscopy with a charge-coupled device (CCD) camera.

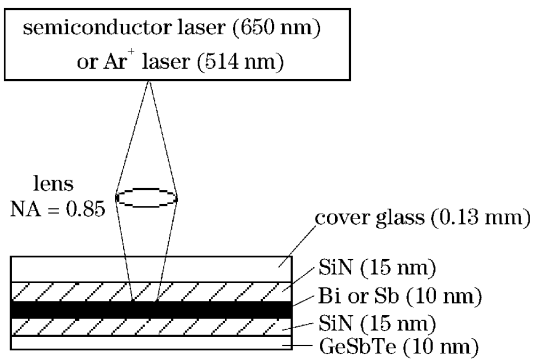

Fig. 1. Cross-sectional view of our super-RENS specimen.

High-quality Bi film is difficult to be prepared[13]. Columnar growth, usually observed in films prepared by thermal evaporation or magnetron sputtering, leads to surface roughness. We optimized the experimental parameters according to the AFM results to obtain high-quality Bi films with small roughness and appropriate film thickness. The mean roughness is less than 1.9 nm for a 10-nm-thick film in our experiments (as shown in Fig. 2). Thicker films have a noticeably rougher surface texture. This result is consistent with Ref. [14]. As-deposited Bi films are also studied by high-resolution grazing incident XRD (as shown in Fig. 3). It is found that when the film is very thin (10 nm), most of the diffraction peaks are very weak, which indicates that it was partly crystalline. The results are consistent with the AFM images shown in Fig. 2. When the film is very thin, it is in the form of discontinuous isolated island. The Sb film of 10-nm thickness in our experiments is amorphous.

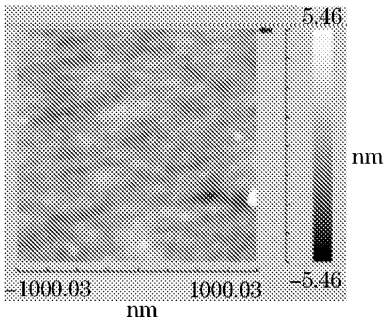

Fig. 2. AFM image of Bi film with thickness of 10 nm.

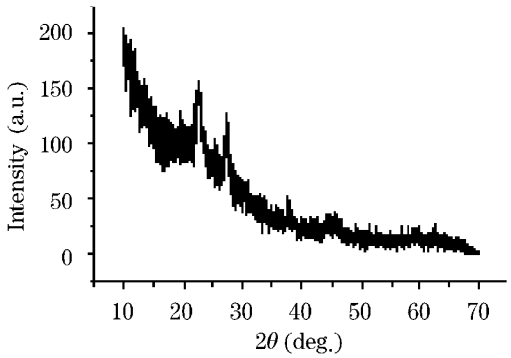

Fig. 3. XRD pattern of as-deposited Bi film with thickness of 10 nm.

Figure 4 shows the optical microscope images marks on single-layered $Ge_2Sb_2Te_5$ film (specimen 4) (a), Sb-super-RENS (specimen 2) (b), and Bi-super-RENS (specimen 3) (c) with power of 14 mW and laser pulse width of 100 ns using a 650-nm semiconductor laser. The diameters of the recording marks on single-layered $Ge_2Sb_2Te_5$ film as shown in Fig. 4(a) are slightly larger than 1 μm. The marks are mostly in dispersive ablated state, only the ambient parts are in crystalline state and the whole marks are not very circular. Figure 4(b) shows the recording marks on $Ge_2Sb_2Te_5$ film with the Sb mask layer. As shown in the optical microscopy images, the diameters of the whole marks are about 1 μm and a much more ablated and smaller aperture, as small as 350−400 nm in diameter, are created in the center of the marks. The relative white part around the aperture is crystalline. The above images show that the Sb mask layer can concentrate the energy into the center of the laser beam and this may be the reason why it can retrieve signals below the diffraction limit. The diameter of the recording marks through the Bi mask layer as shown in Fig. 4(c) are about 1 μm and marks are entirely ablated in this recording condition. Bi film is burned at such high recording power because the melting point of Bi is much lower than that of Sb.

Figure 5 shows the optical microscopy images of the recording marks on single-layered $Ge_2Sb_2Te_5$ film (specimen 4) (a), Sb-super-RENS (specimen 2) (b), and

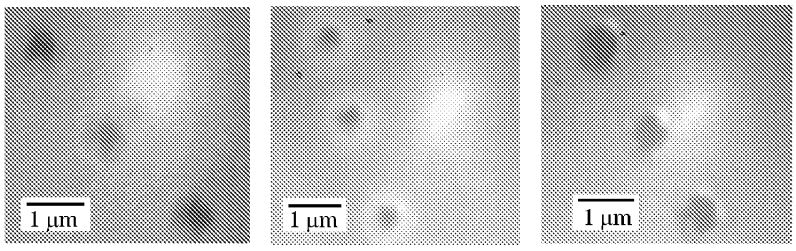

Fig. 4. CCD images of the recording marks on single GeSbTe (a), Sb-super-RENS (b), and Bi-super-RENS (c) with power of 14 mW and laser pulse width of 100 ns using 650-nm semiconductor laser.

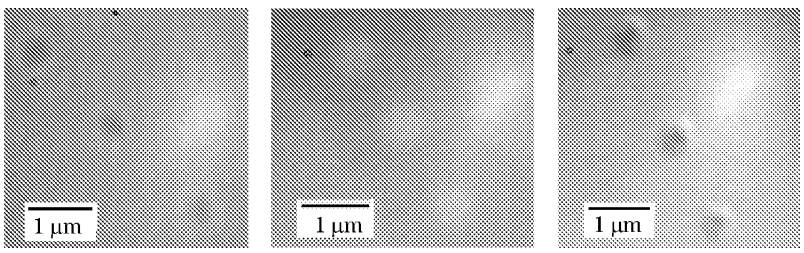

Fig. 5. CCD images of the recording marks on single GeSbTe (a), Sb-super-RENS (b), and Bi-super-RENS (c) with power of 7 mW and laser pulse width of 100 ns using 650-nm semiconductor laser.

Bi-super-RENS (SiN as protection layer, specimen 3) (c) with recording power of 7 mW and laser pulse width of 100 ns using a 650-nm semiconductor laser. As can be seen from Fig. 5(a), the diameters of recording marks on the single-layered $Ge_2Sb_2Te_5$ film are about 0.9 μm and the central ablated part is about 0.5–0.6 μm in diameter. The ambient part is crystalline. The diameters of recording marks through the Sb mask layer shown in Fig. 5(b) are about 0.5 μm, and the marks are entirely crystalline, and no ablated part is formed. Figure 5(c) shows the marks through the Bi mask layer and the SiN protection layer. The diameters of the whole marks are slightly smaller than 0.5 μm and the central part, which is as small as 200 nm and cannot be very clearly distinguished by our optical microscopy system, is more ablated, while parts around the center are less ablated. In conclusion, the Bi mask layer can also concentrate energy into the center of the laser beam at low laser power similar to the Sb mask layer. The transmittance of a 10-nm-thick Bi film is only about 20% at 650 nm. Considering the absorption and reflection of cover glass and two protective layers, the power reaching the $Ge_2Sb_2Te_5$ recording layer is only about 1 mW for a recording power of 7 mW. At such low recording power, the $Ge_2Sb_2Te_5$ film could not be ablated normally. However, the $Ge_2Sb_2Te_5$ film was ablated in our experiments. It is maybe because Bi films could enhance the intensity of the incident laser in the near-field just like Sb films and the reduction of recording marks should not be mainly due to the absorption of the multi-layer.

Figure 6 shows the SEM images of the recording marks on single GeSbTe (specimen 4) (a) and Bi-super-RENS (specimen 3) (b) with recording power of 7 mW and laser pulse width of 100 ns using a 514-nm Ar^+ laser. As can be seen from Fig. 5(a), the diameters of the ablated recording marks on the single-layered $Ge_2Sb_2Te_5$ film is about 800 nm while the size with Bi-super-RENS is only 300 nm. The experimental results in this recording system further prove that Bi mask layer can also concentrate energy into the center of a laser.

Bi is a kind of material with large third-order nonlinear susceptibility $\chi^{(3)}$. Its dominant nonlinear mechanism is regarded as electron-hole plasma during optical heating, which leads to a modulation of the free carrier contributing to the dielectric constant[10,11]. Bi is a semimetal with nearly zero (0.038 eV) energy gap which favors a large $\chi^{(3)}$ since it minimizes the optical energy required to generate each additional electron-hole pair. The electrons and holes in Bi will be easily generated in pairs under laser irradiation. Surface plasma oscillation at the Bi/SiN interface is stimulated by the laser, and then an enhanced field may result from the surface plasma oscillation.

The Bi layer in our super-RENS is about 10 nm thick, which is formed in the isolated island and only partly crystalline. The diffusion of light-generated carriers can be regarded to be slow and can be ignored as in amorphous Sb thin film. The incident field (E_0) and the light field through Bi-super-RENS (E_s) can be regarded as[5]

$$E_0(r) = E_{\max}\exp[-(r/r_0)^2] = \mathrm{sqrt}[2P/(c\varepsilon_0\varepsilon_r\pi r_0^2)]\exp[-(r/r_0)^2], \quad (1)$$

$$E_s(r) = \gamma(\omega)[n_0E_0(r) + \alpha(\omega)\beta(\omega)E_0(r)^3], \quad (2)$$

in which

$$\gamma(\omega) = e^2/(\varepsilon_0\varepsilon_r m_e|\omega^2 - \omega_p^2|), \quad (3)$$

$$\beta(\omega) = [c\varepsilon_0\varepsilon_r\eta\tau_n/(2\hbar\omega)], \quad (4)$$

where P is the power of incident laser, r_0 is the Gauss radius, c is the velocity of light, ε_0 is the permittivity of vacuum, ε_r is the relative permittivity, n_0 is the concentration of equilibrium carriers before laser irradiating, $\alpha(\omega)$ is the absorption coefficient at frequency of ω, η is the dimensionless quantum yield, and τ_n is the lifetime of the light-generated carrier.

We set typical values of Ar^+ laser system, $n_0 = 3\times10^{23}$ m^{-3}, $\eta = 1$, $\tau_n = 1\times10^7$ s, $\varepsilon_r = 10$, $\alpha(\omega) = 7\times10^7$ m^{-1}, λ= 514 nm, NA = 0.85, and $r_0 \approx 0.6$ μm. Calculated incident field (E_0) and light field through Bi-super-RENS (E_s) are show in Fig. 7. It reveals that the third-order nonlinear response of surface plasmas in Bi super-RENS can enhanced the light intensity and reduce the full-width at half-maximum (FWHM) of the beam. The results are in agreement with the experimental results.

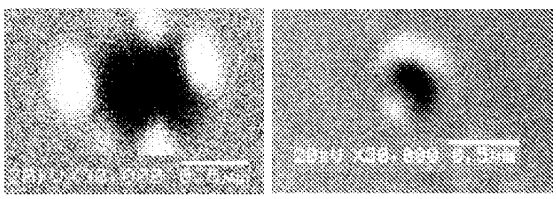

(a) (b)

Fig. 6. SEM images of the recording marks on single GeSbTe (a) and Bi-super-RENS (b) with recording power of 7 mW and laser pulse width of 100 ns using Ar^+ laser.

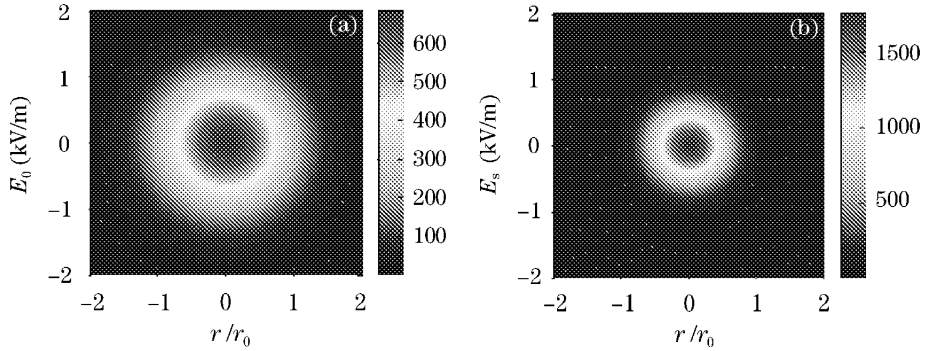

Fig. 7. Calculated results of incident field (E_0) and enhanced field (E_s) through Bi-super-RENS at laser power of 7 mW.

Static recording properties of super-RENS with Bi and Sb as the mask layers were studied and compared using high-resolution optical microscopy with a CCD camera and SEM. The results showed that the Bi mask layer can also concentrate energy into the center of the laser beam at low laser power similar to the Sb mask layer. The third-order nonlinear response induced by the plasma oscillation at the Bi/SiN interface during laser irradiation can be used to explain the phenomenon. The calculation results were basically consistent with our experimental results. Because Bi showed significant optical nonlinearity at low laser power intensity, it could be used in other low-power nonlinear switch applications, except in super-RENS optical storage.

This work was supported by the National "863" Project of China (No. 2002AA313030), the National Natural Science Foundation of China (No. 60207005), and Science and Technology Committee of Shanghai (No. 022261045, 03QG14057). D. Zhang's email is zhfeng0612@siom.ac.cn.

References

1. J. Tominaga, T. Nakano, and N. Atoda, Appl. Phys. Lett. **73,** 2078 (1998).
2. J. Li, H. Ruan, and F. Gan, Chin. J. Lasers (in Chinese) **29**, 366 (2002).
3. T. Fukaya, J. Tominaga, T. Nakano, and N. Atoda, Appl. Phys. Lett. **75,** 3114 (1999).
4. D. P. Tsai and W. C. Lin, Appl. Phys. Lett. **77,** 1413 (2000).
5. D. R. Ou, J. Zhu, and H. Zhao, Appl. Phys. Lett. **82,** 1521 (2003).
6. J. Wei and F. Gan, Appl. Phys. Lett. **82,** 2607 (2003).
7. Y. Liu, K. A. Mcgreer, B. Nease, D. B. Haviland, G. Martinez, J. W. Halley, and A. M. Geldman, Phys. Rev. Lett. **67,** 2068 (1991).
8. F. Y. Yang, K. Liu, K. Hong, D. H. Reich, P. C. Searson, and C. L. Chien, Science **284,** 1335 (1999).
9. E. I. Rogacheva, S. N. Grigorov, O. N. Nashchekina, S. Lyubchenko, and M. S. Dresselhaus, Appl. Phys. Lett. **82,** 2628 (2003).
10. E. R. Youngdale, J. R. Meyer, C. A. Hoffman, F. J. Bartoli, D. L. Partin, C. M. Thrush, and J. P. Heremans, Appl. Phys. Lett. **57,** 336 (1990).
11. Z. Pan, S. H. Morgan, D. O. Henderson, S. Y. Park, R. A. Weeks, R. H. Magruder, and R. A. Zuhr, Optical Materials **4,** 675 (1995).
12. D. R. Liu, K. S. Wu, M. F. Shih, and M. Y. Chern, Opt. Lett. **27,** 1549 (2002).
13. T. Missana and C. N. Afonso, Appl. Phys. A **62,** 513 (1996).
14. R. Atkinson and P. H. Lissberger, Thin Solid Films **7,** 207 (1973).